Optik 152 (2018) 136–145

Contents lists available at ScienceDirect

Optik

journal homepage: www.elsevier.de/ijleo

Original research article

Design and optimization of silicon quantum dot antireflection coating performance for UV spectrum

Asmiet Ramizy[a,b,*], Bashar M. Salih[a], Saeed Naif Turki Al-Rashid[c]

[a] Physics Department, College of Sciences, University of Anbar, Anbar, Iraq
[b] Renewable Energy Research Center, University of Anbar, Anbar, Iraq
[c] Physics Department, Education College for Pure Sciences, University of Anbar, Anbar, Iraq

ARTICLE INFO

Article history:
Received 26 October 2016
Received in revised form 8 September 2017
Accepted 28 September 2017

Keywords:
Quantum dot
Reflectivity
Design
Coating
Silicon

ABSTRACT

In this study, the optical properties of silicon quantum dot as a function of particle size were calculated and investigated. The antireflection coating performance for the spectrum range of 300–400 nm was designed and optimized using MATLAB version 7.11. Results show that the reflectivity of surface decreases from 30.2% to 0.4003% when the size of bulk silicon particle decreases from 40 nm to 2.2 nm. Moreover, the reflectivity of the designed single-layer (Air/Nano Si/Si bulk) is 0.2443% at the incident angle of 0° with wavelength of 350 nm and particle size of 2.6 nm. For the designed (Air/Nano Si/Al_2O_3), reflectivity is 1.3272% at the incident angle of 0° with wavelength of 350 nm and particle size of 2.4 nm. Silicon quantum dot is an excellent antireflection coating against incident light when compared with other antireflection coatings. This material also exhibits good light trapping of wide wavelength spectrum and can thus be used in producing high-efficiency devices.

1. Introduction

Nanostructures can be used in modifying the electronic properties of many nanoscale devices. The electrons in bulk materials can move in three directions. Meanwhile, the properties of electrons in nanostructures can be determined by the effects of quantum confinement. The nanostructures that are designed with two-dimensional, one-dimensional, and zero-dimensional electron motion are called quantum wells, quantum wires, and quantum dots. These impressive examples of manipulating the properties of the current-carrying particles fundamentally illustrate new possibilities for electronics that become viable at the nanoscale [1].

Semiconductor quantum dots are essentially tiny zero-dimensional crystals with size in the order of nanometers [2] and interactions similar to those of bulk semiconductor materials. Their electronic and optical properties are closely related to the size and shape of the individual crystal. Quantum dots are advantageous in that their size can be easily tuned for many applications. Large quantum dots present more significant spectrum shift toward the red direction and exhibit less pronounced quantum properties compared with small dots. Conversely, small particles result in subtle quantum effects [3]. Small crystal size generally generates large band gap energy. When the difference in energy is significant between the highest valence band and the lowest conduction band, much energy is needed to excite the dot and the crystal returns to

* Corresponding author at: Physics Department, College of Sciences, University of Anbar, Anbar, Iraq.
E-mail address: asmat_hadithi@yhaoo.com (A. Ramizy).

https://doi.org/10.1016/j.ijleo.2017.09.107
0030-4026/

its ground state [4]. Quantum dots also exhibit large quantum yield (i.e., percentage of the absorbed photons from emitted photons) and are thus being studied for use in effective solar cells [5].

The present work aims to study and calculate the change in optical properties of silicon as a function of particle size, and design and optimize the antireflection coating performance for the spectrum range of 300–400 nm. The novelty and motivation of our work is to study of ultraviolet radiation range of incident light with wavelength between (300nm–400 nm) which utilized in space applications not just for earth applications.

2. Theoretical basis

2.1. Brus equation

When the sizes (Ps = 2R) of the nanoparticles become comparable to or smaller than the Bohr exciton radius (α_B), a quantum confinement effect is expected from these particles. In these materials, the electrons are confined in three directions and become the optical properties of material associated with particle size. Such a system is called a zero-dimensional system, which is evident in quantum dots [1,6]. The Bohr radius is given by

$$\alpha_B = \frac{4\pi\varepsilon\hbar^2}{e^2}\left[\frac{1}{m_e^*}+\frac{1}{m_h^*}\right], \tag{1}$$

where ε is the dielectric constant. $m_e{}^*$ and $m_h{}^*$ are the effective masses of electrons and holes, respectively.

Different theoretical models can be used in understanding the variation in band gap with particle size; the most commonly used method is effective mass approximation (EMA), in which the variation in excitation energy with particle size is predicted for estimating the crystalline size [7]. In the present study, the EMA model was used in estimating the particle size.

According to the EMA model, the lowest excited state of crystallite is the ground state of an electron hole pair. The ground state energy of exciton or the increase in effective band gap as a function of crystalline size is given by [8]:

$$E_g^{\text{nano}}(R) = E_g^{\text{bulk}} + \frac{\hbar^2\pi^2}{2R^2}\left[\frac{1}{m_e^*}+\frac{1}{m_h^*}\right] - \frac{1.786e^2}{\varepsilon R}, \tag{2}$$

Where $E_g^{\text{nano}}(R)$ is the effective bandgap, E_g^{bulk} is the bulk bandgap, and R is the radius of the particles. The second term on the right hand side shows that the effective band gap is inversely proportional to R^2 and increases as size decreases. The third term shows that the band gap energy decreases with the decrease in R because of the increase in Columbic interaction force. However, given that the second term becomes dominant with small R, the effective band gap is expected to increase with the decrease in R, especially when R is small. The Columbic interaction force is typically small compared with quantum confinement. The third term is much smaller than the first term. Therefore, these terms can be neglected. Thus, the equation may be expressed as [4]:

$$E_g^{\text{nano}}(R) = E_g^{\text{bulk}} + \frac{\hbar^2\pi^2}{2R^2}\left[\frac{1}{m_e^*}+\frac{1}{m_h^*}\right] \tag{3}$$

2.2. Refractive index and energy band

Refractive index is closely related to the energy band structure of the material; many attempts have been made to relate refractive index and energy gap (E_g) through simple relationships [9–14]. However, these relationships of n are independent of temperature and incident photon energy. In [14], the various relationships between n and E_g are reviewed. Different relationships are also suggested between the band gap and the high-frequency refractive index, and a linear form of n as is presented as a function of E_g:

$$n = \alpha + \beta E_g, \tag{4}$$

where $\alpha = 4.048 \& \beta = -0.62\ \text{eV}^{-1}$

Considering the simple physics of light refraction and dispersion, an empirical relationship is proposed as [15]

$$n = 1 + \sqrt{\left(\frac{A}{E_g+B}\right)^2} \tag{5}$$

where $A = 13.6$ eV and $B = 3.4$ eV [16]. Another approach for solving the problem is through considering the band structural and quantum–dielectric formulations [17,18]. By introducing A as the contribution from the valence electrons and B as a constant additive to the lowest band gap E_g, the expression for the high-frequency refractive index is written as

$$n^2 - 1 = \frac{A}{\left(E_g+B\right)^2}, \tag{6}$$

Where $A = 25E_g + 212$, $B = 0.21E_g + 4.25$, and (E_g + B) refers to an appropriate average energy gap of material.

2.3. Characteristic matrix

The amplitude of the reflected wave at the interface between the substrate and the incident media is proportional to the Fresnel amplitude reflection coefficient r [19]:

$$r = \frac{\eta_\circ - \eta_1}{\eta_\circ + \eta_1}, \tag{7}$$

where $\eta_\circ$ is the optical admittance or the effective refractive index of the incident medium and η_1 is the refractive index of the substrate.The reflectance R is given by [20]

$$R = rr^* = \left(\frac{\eta_\circ - \eta_1}{\eta_\circ + \eta_1}\right)\left(\frac{\eta_\circ - \eta_1}{\eta_\circ + \eta_1}\right)^* \tag{8}$$

When plane electromagnetic wave is normal incident to the surface, the optical admittance is equal to the refractive index n if the reflectance R is given as

$$R = \left(\frac{n_\circ - n_1}{n_\circ + n_1}\right)^2 \tag{9}$$

Meanwhile, at oblique incidence,

$$\eta_p = n/\cos\theta, \tag{10}$$

$$\eta_s = n\cos\theta, \tag{11}$$

Where, η_p is the optical admittance for P-Polarization and $\eta_s$is the optical admittance for S-Polarization.

For a system consisting of one layer of thin film on substrate, the characteristic matrix is given by

$$\begin{bmatrix} B \\ C \end{bmatrix} = \begin{bmatrix} \cos\delta & i\sin\delta/\eta_1 \\ i\eta_1\ \sin\delta & \cos\delta \end{bmatrix} \begin{bmatrix} 1 \\ \eta_{\text{sub}} \end{bmatrix}. \tag{12}$$

For a system consisting of several layers (q), the characteristic matrix is given by [21]

$$\begin{bmatrix} 1 \\ Y \end{bmatrix} = \left\{ \prod_{r=1}^{q} \begin{bmatrix} \cos\delta_r & i\sin\delta_r/\eta_r \\ i\eta_r\sin\delta_r & \cos\delta_r \end{bmatrix} \right\} \begin{bmatrix} 1 \\ \eta_{\text{sub}} \end{bmatrix}. \tag{13}$$

The square matrix (2×2) on the right hand side describes the characteristics of each film and the angle of incidence and polarization pattern.

Where, $\delta_r = 2\pi n_r d_r \cos\theta_r/\lambda$

$n_r d_r$: optical thickness for layer.

A useful property of the characteristic matrix of thin film is that the determinant is in unity. Therefore, the determinant of the product of any number of these matrices is also in unity. The multilayer can be replaced by a single surface, which presents an input optical admittance ($Y = B/C$). Eq. (13) includes all information for assembly of multilayer, and reflectivity and transmittance can be obtained for oblique incident of wave from the following equation [20]:

$$R = \left(\frac{\eta_\circ B - C}{\eta_\circ B + C}\right)\left(\frac{\eta_\circ B - C}{\eta_\circ B + C}\right)^*. \tag{14}$$

$$T = \frac{4\eta_\circ Re\,(\eta_{\text{sub}})}{(\eta_\circ B + C)(\eta_\circ B + C)^*}. \tag{15}$$

3. Results and discussion

Acomputer program using MATLAB version7.11was design for studying and calculatingthe change in optical properties of silicon as a function of particle size.The program was also used fordesigning and optimizing the antireflection coating performance for the spectrum range of 300–400 nm. The programming is based on the using of Matlab to construct a set of mathematical functions that are used to calculate the optical properties of the designs as function of the coating material particle size and the wavelength of the incident light respectively. The programs set up are based on several Eqs. (3), (4), (8) and (13). Eq. (4) was adopted because it achieved good agreement with the experimental work by (Asmiet Ramizy et al.) [22]. By using these equations the optical characteristics of the design calculated according to the input data such as, Layers No, refractive indices for base and coatings material, incident angle, electron and hole Effective mass and energy gap for the optical coatings materials are used. Figs. 1 and 2 was illustrated the coatings that were designed in this study.

Figs. 3–6 show the change in optical properties of silicon as a function of particle size. The optical properties of silicon are affected by the decrease in particle size. Specifically, when particle size approaches to the Bohr exaction radius ($\alpha_B = 4.3$ nm), the energy gap increases but refractive index and reflectivity decrease. This result is due to the effect of quantum confinement.

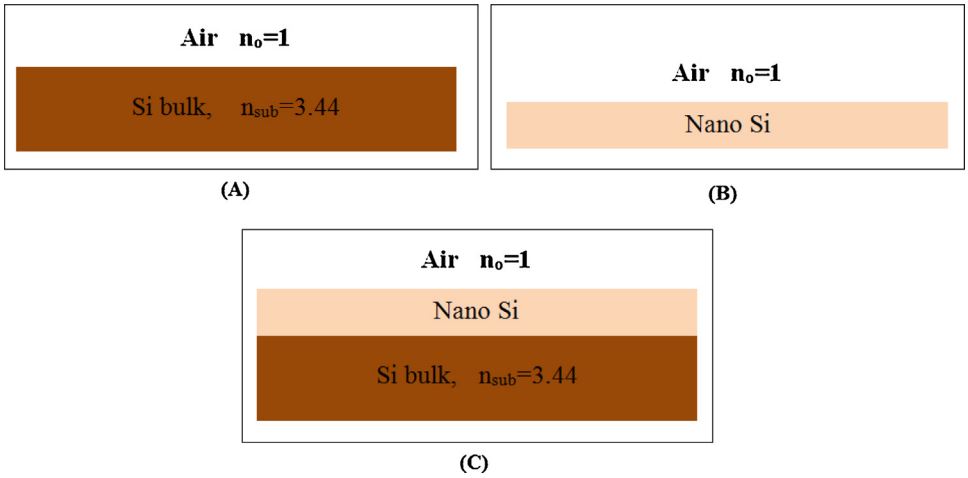

Fig. 1. (A) (Air/Si bulk), refractive index for the air (no = 1), refractive index for substrate (n_1 = 3.44). (B) (Air/Nano Si),refractive index of the air (no = 1), λ_o = 350 nm, L = 0.25λ_o. (C) (Air/Nano Si/Si bulk),refractive index of the air (no = 1), refractive index for substrate (n1 = 3.44),Ps_{nanoSi} = 2.6 nm, λ_o = 350 nm, L = 0.25λ_o.

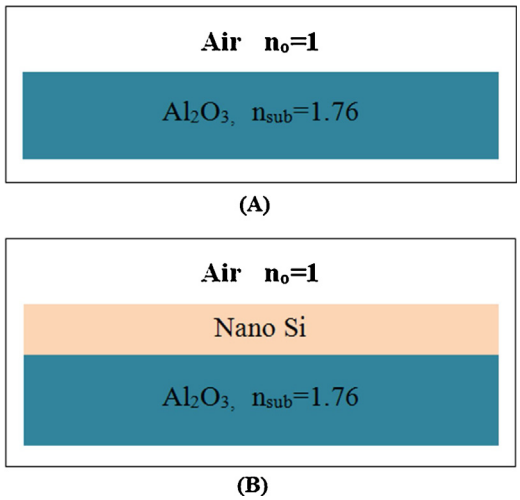

Fig. 2. (A) (Air/Al_2O_3), refractive index for the air (no = 1), refractive index of substrate (n_1 = 1.76). (B) (Air/Nano Si/Al_2O_3),refractive index of the air (no = 1), refractive index of substrate (n1 = 3.44), Ps_{nanoSi} = 2.6 nm, λ_o = 350 nm, L = 0.25λ_o.

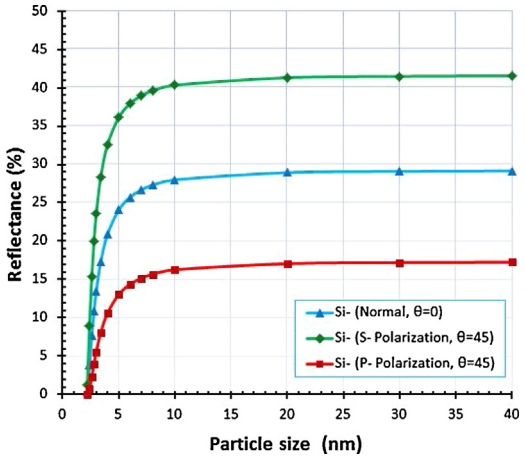

Fig. 3. Reflectance as a function of particle size of silicon from air, at incident angle (θ = 0°) and (θ = 45°).

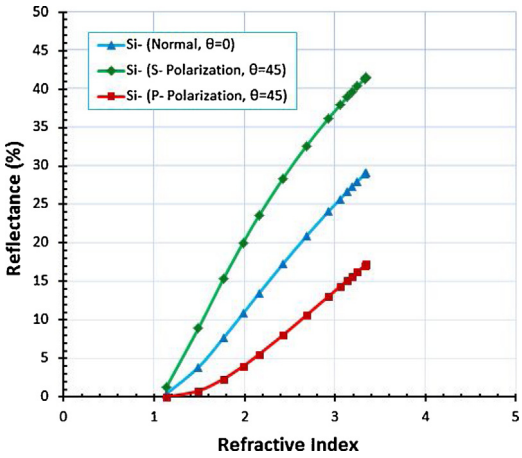

Fig. 4. Reflectance as a function of refractive index of silicon from air, at incident angle ($\theta = 0^{\circ}$) and ($\theta = 45^{\circ}$).

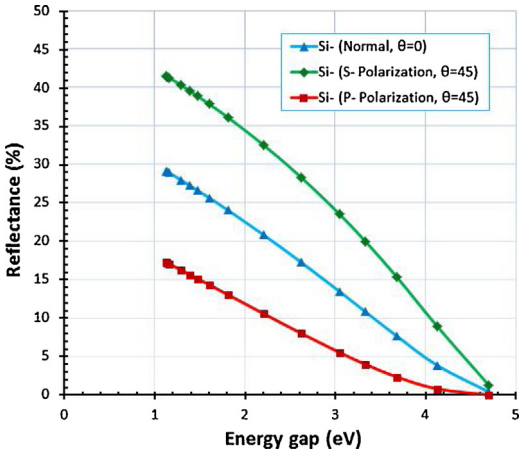

Fig. 5. Reflectance as a function of energy gap of silicon from air, at incident angle ($\theta = 0^{\circ}$) and ($\theta = 45^{\circ}$).

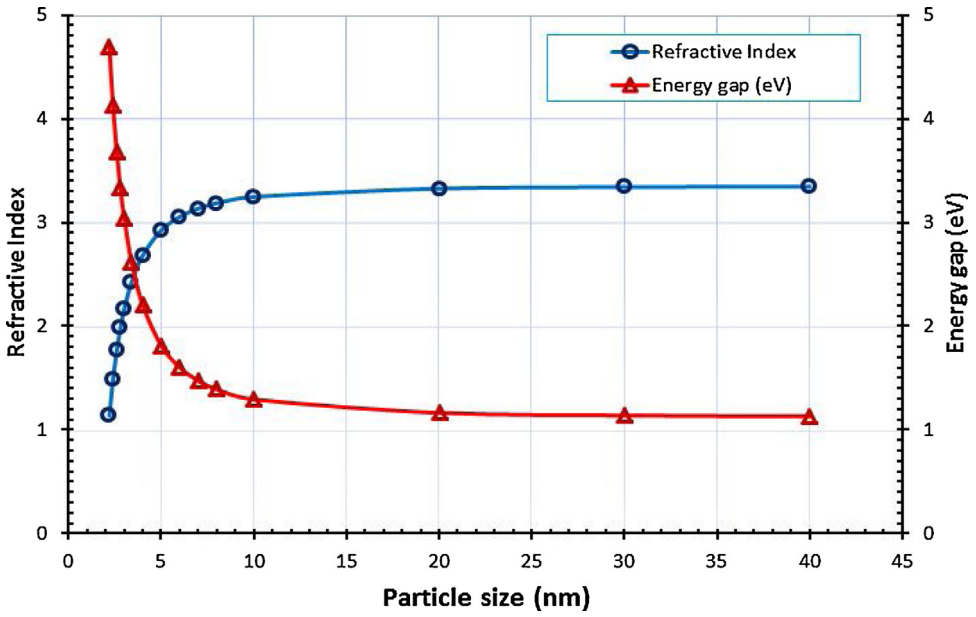

Fig. 6. Refractive index and the energy gap as a function of particle size of silicon from air.

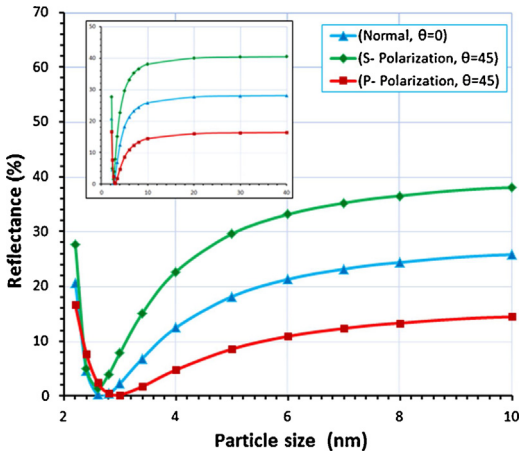

Fig. 7. Reflectance as a function of particle size of the design (Air/Nano Si/Si bulk), n_{sub} = 3.44, at λ_o=350 nm, L = 0.25λ_o, at incident angle (θ = 0°) and (θ = 45°).

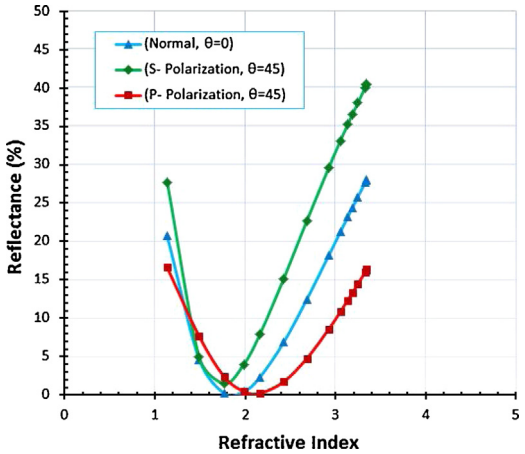

Fig. 8. Reflectance as a function of refractive index of the design (Air/Nano Si/Si bulk), n_{sub} = 3.44, at λ_o = 350 nm, L = 0.25λ_o, at incident angle (θ = 0°) and (θ = 45°).

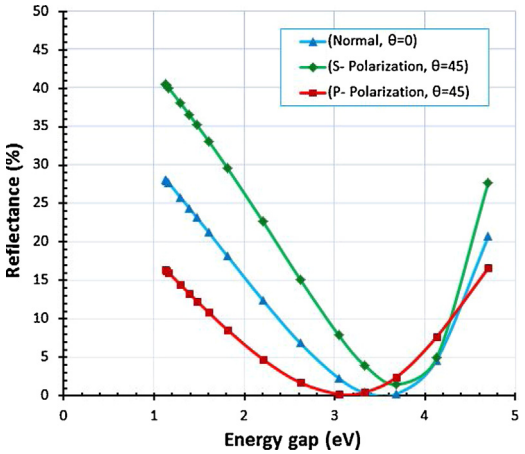

Fig. 9. Reflectance as a function of energy gap of the design (Air/Nano Si/Si bulk), n_{sub} = 3.44, at λ_o = 350 nm, L = 0.25λ_o, at incident angle (θ = 0°) and (θ = 45°).

When particle size (Ps = 2R) is equal or smaller than the Bohr exciton radius, the effect of quantum confinement increases dramatically, there by significantly decreasing reflectivity and refractive index of material [22,23].

Figs. 7–9 show the optical properties of the designed antireflection layer (Air/Nano Si/Si bulk) as a function of particle size.The reflectivity of Si bulk is 28.1%when particle size is in the range of 20–40 nm. This result agrees with that of other

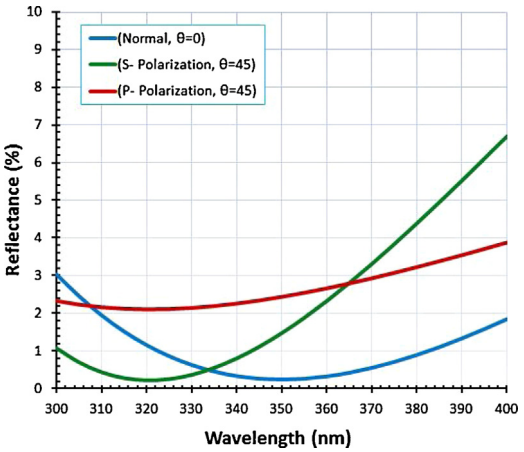

Fig. 10. Reflectance as a function of wavelength for design (Air/Nano Si/Si bulk), $Ps_{nanoSi} = 2.6$ nm, $n_{sub} = 3.44$, $L = 0.25\lambda_o$, $\lambda_o = 350$ nm, at incident angle ($\theta = 0^\circ$) and ($\theta = 45^\circ$).

experimental investigation [22]. The refractive index of the silicon antireflection coating is approaches to silicon substrate refractive index as showed in inset graph in Fig. 7. Thus,the reflectivity of this designed layer is equal to the reflectivity of silicon bulk, however, when the particle size of coating approaches to the Bohr exciton radius, the effect of quantum confinement shows a decrease in reflectivity to 25.7% at the incident angle of 0° with wavelength of 350 nm and particle size of 10 nm.

The decline in the value of reflectivity with low particle size of coating increases significantly when particle size is equal or smaller than the Bohr exciton radius. The minimum reflectivity is 0.244% when the partial size of coating is 2.6 nm. This finding indicates that the particles are confined in low dimension, and the probability of recombination of electrons and holes is high in low-dimensional structures. Accordingly, the structures exhibit high-emission efficiency because of the effects of quantum confinement [24]. Therefore, the silicon with nanoparticle size of 2.6 nm and thickness of a quarter waves can be used as an antireflection coating performance for the spectrum range of 300–400 nm. When the particle size of coating become smaller than 2.6 nm, refractive index decreases dramatically and approaches to the refractive index of air. Moreover, its effect on the reflectivity of the designed layer is low or negligible, thereby increasing reflectivity again.

The successfully designed single-layer (Air/Nano Si/Si bulk) is shown in Fig. 10. This designed layer presents particle size of 2.6 nm and reflectivity of 0.2443% at the incident angle f 0° when the thickness of layer equals a quarter wave at λ_o in the spectrum range of 300–400 nm. The maximum and maximum reflectance of 3.03% and 0.2443% are observed at the incident angle of 0°. At the incident angle of 45°, the reflectance ($R = 1.4744\%$ for S-Polarization and $R = 2.4338\%$ for P-Polarization) is at a quarter wave thickness at λ_o. The center wavelength shifts toward the shorter wavelengths. The shift of the center wavelength can be accurately quantified using a simple model of the center wavelength λ versus the angle of incidence θ. This dependence can be accurately described by the following expression [25]:

$$\lambda = \lambda_\circ \sqrt{1 - sin^2\theta/\eta^2},$$

where λ_o is the central wavelength at normal incidence, θ is the angle of incidence, and η is the effective refractive index inside the coating.

The angle-induced changes can be qualitatively divided into (1) the wavelength shift and (2) the polarization effects.

Wavelength shifts to shorter wavelengths (in the blue direction) as the angle of incidence moves from the normal. Initially, the performance shifts toward the red direction because the optical thickness of each of the layers in the design increases as the angle of incidence increases (by a factor inversely proportional to the cosine of the angle of refraction inside the layer). However, the important parameter is not the total phase shift introduced in the waves by the layers but rather the phase difference between the waves reflected from all of the interfaces into the summation of the partial reflected waves. For normal incidence ($\theta = 0^\circ$),polarization does not influence reflectivity. Increasing the angle of incidence leads to a split of the reflectivity characteristics for the S- and P-polarized beams. This split becomes evident for incident angles larger than approximately 15°. Furthermore, at oblique angles ($\theta = 0^\circ$), the reflectivity band shifts toward shorter wavelengths [26,27].

The result of layer coating of nano silicon with thickness of a quarter wave on the sapphire substrate shows a very low reflectivity when the particle size is smaller or equal to 2.4 nm (Figs. 11–13). When particle size increases, the refractive index of coating increases dramatically and the reflectivity of design also increases. Therefore, the coating of silicon with particle size of 2.4 nm with thickness of a quarter wave on the sapphire substrate is a promising antireflection coating performance for the spectrum range of 300–400 nm.

Fig. 14 shows the successfully designed single-layer (Air/Nano Si/Al_2O_3)with particle size of 2.4 nm. For the spectrum range of 300–400 nm, the maximum reflectance is 1.7725% at wavelength of 300 nm and the minimum reflectance is 1.3272% at a quarter wave thickness at $\lambda_o = 350$ of the incident angle of 0°. At the incident angle of 45°, the reflectance ($R = 4.5383\%$

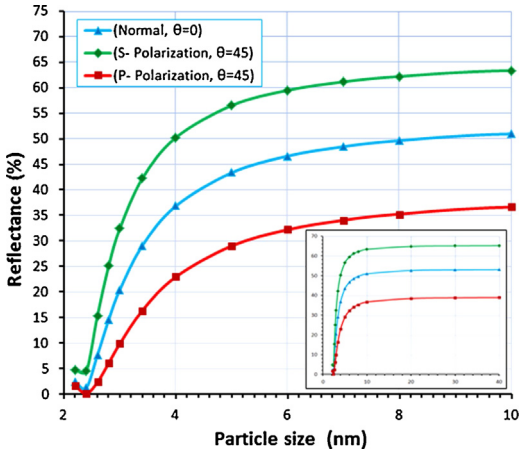

Fig. 11. Reflectance as a function of particle size of the design (Air/Nano Si/Al_2O_3), n_{sub} = 3.44, at λ_o = 350 nm, L = 0.25λ_o, at incident angle ($\theta = 0^\circ$) and ($\theta = 45^\circ$).

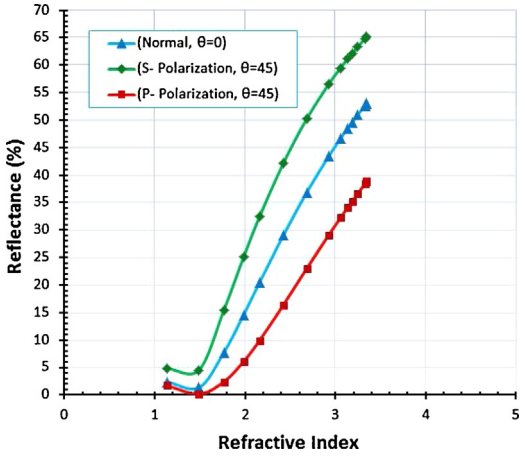

Fig. 12. Reflectance as a function of refractive index of the design (Air/Nano Si/Al_2O_3), n_{sub} = 3.44, at λ_o = 350 nm, L = 0.25λ_o, at incident angle ($\theta = 0^\circ$) and ($\theta = 45^\circ$).

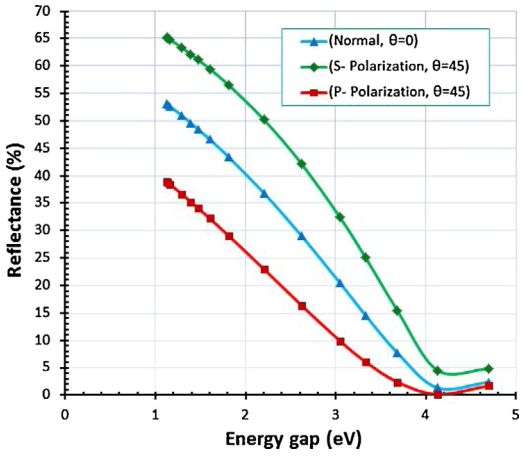

Fig. 13. Reflectance as a function of energy gap of the design (Air/Nano Si/Al_2O_3), n_{sub} = 3.44, at λ_o = 350 nm, L = 0.25λ_o, at incident angle ($\theta = 0^\circ$) and ($\theta = 45^\circ$).

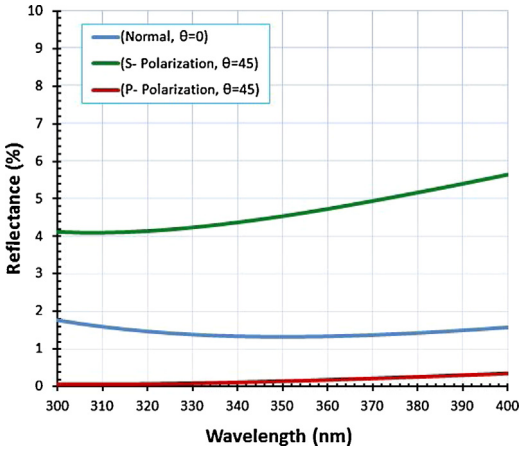

Fig. 14. Reflectance as a function of wavelength for design (Air/Nano Si/Al_2O_3), Ps_{nanoSi} = 2.4 nm, n_{sub} = 3.44, L = 0.25λ_o, λ_o = 350 nm, at incident angle ($\theta = 0^\circ$) and ($\theta = 45^\circ$).

Table 1
The values of Reflectivity coating Nano Si of the substrate (Si bulk, Al_2O_3) for incident angles (0°, 45°).

Number of Figure	The design	Particle size of the coating (Ps) nm	Incidence angle	Reflectivity R
8	(Air/Nano Si/Si bulk)	2.6	0 45	R = 0.2443 R_S = 1.4744 R_P = 2.4338
13	(Air/Nano Si/Al_2O_3)	2.4	0 45	R = 1.3272 R_S = 4.5383 R_P = 0.1487

for S-Polarization and $R = 0.1487\%$ for P-Polarization) is at a quarter wave thickness at λ_o. This result shows that reflectivity shifts toward shorter wavelengths, as discussed earlier. Table 1 included the optimum reflectivity result of the coating layers designed.

4. Conclusion

The reflectivity of antireflection coating layer within the ultraviolet region of 300–400 nm depends on the refractive index of coating and angle of incidence. The value of refractive index can be controlled through particle size. The antireflective coating of a single layer with nanoparticle size shows more efficient in reducing the reflection of electromagnetic radiation than with bulk dimensions coatings, the best coating is one layer of Si nano with particle size of 2.6 nm. This design obtains the lowest reflection of $R = 0.2443\%$ at $\theta = 0^\circ$, and $R = 1.4744$ for S-Polarization and $R = 2.4338\%$ for P-Polarization at $\theta = 45^\circ$. These properties are promising for solar cell application. On Al_2O_3 substrate, the best coating is one layer of Si nano with particle size of 2.4 nm. This design obtains the lowest reflection of $R = 1.3272\%$ at $\theta = 0^\circ$, and $R = 4.5383$ for S-Polarization and $R = 0.1487\%$ for P-Polarization at $\theta = 45^\circ$. These characteristics are promising for optical detection application.

Acknowledgment

Authors are grateful to the Physics Department, College of Sciences, University of Anbar, Anbar, Iraq.

References

[1] Vladimir V. Mitin, Viatcheslav A. Kochelap, Michael A. Stroscio, Introduction to Nanoelectronics Science, Nanotechnology, Engineering and Applications, Cambridge University Press, 2008 (pp. 6).
[2] R.D. Schaller, V.I. Klimov, High efficiency carrier multiplication in PbSe nanocrystals: implications for solar energy conversion, Phys. Rev. Lett. 92 (18) (2004), 186601, http://dx.doi.org/10.1103/PhysRevLett.92.186601.
[3] C. Wang, M. Shim, P. Guyot-Sionnest, Electrochromic nanocrystal quantum dots, Science 291 (5512) (2001) 2390–2392, http://dx.doi.org/10.1126/science.291.5512.2390.
[4] E. Chukwuocha, M. Onyeaju, T. Harry, Theoretical studies on the effect of confinement on quantum dots using the Brus equation, World J. Condens. Matter Phys. 2 (2) (2012) 96–100, http://dx.doi.org/10.4236/wjcmp.2012.22017.
[5] O. Yoshitaka, "Solar Quest" Nature Photonics Technology Conference, Tokyo, 19–21 October, 2010.
[6] M.A. Mahdi, Z. Hassan, S.S. Ng, J.J. Hassan, S.K. MohdBakhori, Structural and optical properties of nanocrystalline CdS thin films prepared using microwave-assisted chemical bath deposition, Thin Solid Films (2012) 3477–3484.
[7] Shashank Sharma, Ravi Sharma, Study on th optical properties of MN doped ZnS nanocrystals, Int. Sci. J. 2 (1) (2015) 120–130.

[8] Zhong Lin Wang, Yi Liu, Ze Zhang, Handbook of Nanophase and Nanostructured Materials, vol. II, Kluwer Academic Plenum, 2003 (ISBN: 9780306472497).
[9] T.S. Moss, A relationship between the refractive index and the infra-red threshold of sensitivity for photoconductors, Proc. Phys. Soc. B 63 (1950) 167.
[10] V.P. Gupta, N.M. Ravindra, Comments on the Moss formula, Phys. Status Solidi B 100 (1980) 715.
[11] Y. Al-Douri, Electronic and optical properties of ZnxCd1-xSe, Mater. Chem. Phys. 82 (2003) 49.
[12] Y. Al-Douri, Y.P. Feng, A.C.H. Huan, Optical investigations using ultra-soft pseudopotential calculations of Si0.5Ge0.5 alloy, Solid State Commun. 148 (2008) 521.
[13] P. Hervé, L.K.J. Vandamme, General relation between refractive index and energy gap in semiconductors, Infrared Phys. Technol. 35 (1994) 609.
[14] N.M. Ravindra, S. Auluck, V.K. Srivastava, On the Penn Gap in Semiconductors, Physica status solidi (b) 93 (1979).
[15] P.J.L. Herve, L.K.J. Vandamme, Empirical temperature dependence of the refractive index of semiconductors, J. Appl. Phys. 77 (1995) 5476.
[16] D.K. Ghosh, L.K. Samanta, G.C. Bhar, A simple model for evaluation of refractive indices of some binary and ternary mixes crystals, Infrared Phys. 24 (1984) 34.
[17] D.R. Penn, Wave-number-dependent dielectric function of semiconductors, Phys. Rev. 128 (1962) 2093.
[18] J.A. Van Vechten, Quantum dielectric theory of electronegativity in covalent systems I. Electronic dielectric constant, Phys. Rev. 182 (1969) 891.
[19] R.R. Willely, Practical Design and Production of Optical Thin Films, Marcel Dekker, Inc., New York, Basel, 2002.
[20] H. Angus Macleod, Thin-Film Optical Filters, fourth edition, CRC Press, Taylor & Francis Group, LLC, 2010 (ISBN:9781420073027).
[21] E. Bruce Perillouxm, Thin-film Design: Modulated Thickness and Other Stopband Design Methods, SPIE Press, 2002.
[22] Asmiet Ramizy, Z. Hassan, Khalid Omar, Y. Al-Douri, M.A. Mahdi, New optical features to enhance solar cell performance based on porous silicon surfaces, Appl. Surf. Sci. 257 (14) (2011) 6112–6117.
[23] A. Laref, NouraAlshammari, S. Laref, S.J. Luo, Surface passivation effects on the electronic and optical properties of silicon quantum dots, Sol. Energy Mater. Sol. Cells (2013) 622–630.
[24] A. Ramizy, S.H. Abud, A.S. Hussein, Z. Hassan, F.K. Yam, C.W. Chin, Novel InGaN Mesoporous Grown by PA-MBE Materials Science in Semiconductor Processing, 2015, pp. 102–105.
[25] Manuel A. Quijada, Catherine Trout Marb, Richard G. rendt, S. Harvey Moseley, Angle-of-Incidence Effects in the Spectral Performance of the Infrared Array Camera of the Spitzer Space Telescope Optical, Infrared, and Millimeter Space Telescopes, Society of Photo-Optical Instrumentation Engineers (SPIE), Glasgow, Scotland, United Kingdom, 2004, ISSN :0277786X, pp. 244–252.
[26] James D. Rancourt, Optical Thin Films: User Handbook, SPIE Press, 1996 (ISBN:9780819422859).
[27] Friedrich Bachmann, Peter Loosen, Reinhart Poprawe, High Power Diode Lasers: Technology and Applications, Springer, 2007 (ISBN:9780387347295).